Selective determination of poly(styrene) and polyolefin microplastics in sandy beach sediments by gel permeation chromatography coupled with fluorescence detection

Tarita Biver, Sabrina Bianchi, Maria Rita Carosi, Alessio Ceccarini, Andrea Corti, Enrico Manco, Valter Castelvetro*

Department of Chemistry and Industrial Chemistry, University of Pisa, via G. Moruzzi 13, 56124 Pisa, Italy

** Corresponding author: valter.castelvetro@unipi.it*

Tarita Biver and Andrea Corti proposed and participated to the planning, experimentation and writing; Sabrina Bianchi, Maria R. Carosi and E. Manco carried out experimental work, A. Ceccarini supervised the experimental work and V. Castelvetro coordinated the research, provided funding and revised the paper.

Abstract

Plastics waste and the microplastics generated by their degradation are ubiquitous in marine and freshwater basins, posing serious environmental concerns. Raman and FTIR spectroscopies, along with more specialized techniques such as pyrolysis-GC/MS, are typically used for their identification. In this research note we present a procedure for the selective and semi-quantitative determination of the most common polluting microplastics found in marine shoreline sediments: poly(styrene) and partially degraded polyolefins. The analytical procedure is based on gel permeation chromatography (GPC) coupled with fluorescence detection at specific excitation/emission wavelengths enabling selective determination of oxidatively degraded poly(ethylene) (LDPEox) and of poly(styrene) (PS). Dichloromethane extracts of both PS and LDPEox as reference materials yield linear plots of fluorescence peak area vs concentration.

Keywords

Gel permeation chromatography, fluorescence, marine litter, microplastics, polystyrene, polyolefin

Introduction

The increasing attention towards the plastic pollution in water basins and their sediment systems is stimulating efforts aimed at improving sampling and characterization procedures. In this context, the pollution of sediments by microplastics has been scarcely investigated. Microplastics are minute plastics debris and particles with size ranging from few microns to a higher threshold varying, according to different researchers, from 500 μm up to 5 mm.[1] Their dispersion in the environment is a consequence of their presence (as synthetic fibers, microbeads) and release into wastewater, mainly from textile and personal care products, or of the fragmentation of larger plastic items caused by environmental degradation (photo-oxidative, hydrolytic) processes. Commodity hydrocarbon polymers such as polyethylene (PE), polypropylene (PP), and polystyrene (PS) are those more likely to end up in shoreline rather than sea bottom sediments because of their low density. For these polymers environmental degradation occurs mainly through a photochemically assisted generation of oxidized functional groups (carbonyl, carboxyl, hydroxyl) followed by chain scissions and consequent reduction of the average molecular weight. These processes weaken the integrity of plastic items that become brittle up to their powdery disintegration. It has been suggested that these polymers may produce a substantial contribution in the pollution of coastal sediments by microplastics since the processes of degradation and embrittlement of larger items proceed as they float at the sea/freshwater surface, and are accelerated once they are deposited ashore, where photo-oxidative, thermal and mechanical stresses are greater.[2,3] While sampling based on filtration limits the sampling to microplastics larger than 300-500 μm from the water column, in the case of sediments sieving followed by density separation and filtration steps may allow collection and identification of microplastics down to 1-2 μm.[4] However, isolation and characterization of individual small particles is not only impractical but also poorly representative of the diversity of this kind of pollution, also as a consequence of the contamination of microplastics with organic compounds and inorganic particles captured from the environment.[4,5] Chemical and enzymatic pre-treatments, including 30-35% hydrogen peroxide,[6] 30% HCl, and concentrated alkaline (e.g. NaOH) solutions,[5,7] have been employed to remove organic contaminants from the microplastics in coastal sediment samples. Such aggressive chemical agents, however, may cause significant degradation or further alteration of the microplastics present in treated samples.[8]

Among the techniques used for the chemical identification of microplastics separated from sediment samples the most common are Fourier transformed infrared and Raman spectroscopies[4,9] and, for smaller particles, micro-Raman and micro-FT-IR,[10-12] the latter also associated with molecular imaging or focusing tools allowing the collection of spectra during visual inspection of the samples.

Less practical for routine analysis but very effective for the chemical identification of plastics debris and their degradation products is pyrolysis coupled with gas-chromatography-mass spectrometry (Py-GC/MS).[13] Fabbri et al[14] used this technique to assess the contamination with poly(vinyl chloride) and other polymers in bottom sediments of a coastal lagoon, after isolation of the polymeric fractions by solvent extraction and re-precipitation in n-hexane. Direct analysis without polymer isolation suffers from the interference of inorganic components of the sediments affecting the degradation patterns of the polymeric materials during the analysis,[15] and from natural organic matter such as humic compounds whose thermal degradation produced the same congeners of synthetic polymers, particularly styrenic ones.[16, 17] Accordingly, a procedure based on thermal decomposition followed by absorption into a solid-phase device and subsequent GC/MS identification of the pyrolysis and other volatile products has been proposed for the analysis of microplastics in sediments coming from environmental samples of complex composition.[18-19] However, the same factors influencing the Py-GC/MS response may reduce the accuracy and reliability of the latter procedure when bulk sediment samples are analyzed. On the other hand, several interfering factors may also affect the results of FT-IR and Raman spectroscopic analyses, including the morphology of single microplastics fragments,[11] the presence of surface contaminants such as natural compounds, persistent organic pollutants[20] or biofilms.[21,22] Many of the cited methodologies comprise a separation step or the isolation and analysis of single microplastics fragments, limiting the minimum size of the fragment that can be reliably characterized and possibly excluding the extensively degraded ones, which may be more difficult to separate from the inorganic sediment or from biogenic debris.

The present article is intended as a contribution to the improvement of the methodologies and techniques that, if used in a synergistic way, may provide more accurate information about level of contamination and fate of very small size microplastics and relevant degradation products in coastal sediments. In particular, gel permeation chromatography (GPC) equipped with refractive index, ultra violet diode array and spectrofluorometric detectors has been used for qualitative and quantitative analysis of the polymer content in solvent extracts from coastal sediments sampled in a public sandy beach of northern Tuscany (Italy), which had been found to contain mainly low density polymers such as expanded polystyrene, polyethylene and polypropylene along with their partial degradation polymeric and oligomeric species.[3]

Materials and Methods

Two polymeric materials representative of oxidatively degraded poly(ethylene) and poly(styrene) were used as reference compounds: i) the dichloromethane (DCM) soluble fraction of a partially

oxidized low density poly(ethylene) (LDPEox) obtained after 120 days thermal aging in air ventilated oven a 70 °C; ii) a commercial sample of expanded poly(styrene). As the environmental materials, DCM extracts previously collected from shoreline sand samples were analyzed.[3]

Gel permeation chromatography (GPC) analyses were performed with an Agilent 1260 Infinity Binary LC instrument equipped with diode array (DAD VL+ 1260/G1315C) plus fluorescence (FLD 1260/G1321B) double detector, and two in series PLgel MIXED-E Mesopore columns (Polymer Laboratories) thermostated at 30°C, using chloroform at 1.0 mL/min flow rate as the eluent. Ten polystyrene standards with molecular weights ranging from 800 to 300,000 g/mol^{-1} (Polymer Laboratories Ltd. and Varian, Inc.) were used for calibration. Both GPC detectors were calibrated for quantitative determination of the polymeric materials. For this purpose, five DCM solutions of PS (concentration range 0.02-4.15 mg/mL) and three DCM solutions of LDPEox (concentration range 0.54-5.61 mg/mL) were analyzed in triplicate by using the DAD detector at 261 nm and 243 nm, respectively, recording the average peak areas and relevant confidence interval. The same PS and LDPEox solutions were also used to calibrate the FLD detector once checked the most selective excitation and emission wavelengths for each polymeric material.

Fluorescence spectra were separately recorded with a Perkin Elmer LS55 instrument, using reference materials and environmental samples in DCM, previously filtered on 0.2 μm PTFE membrane. Both excitation (wavelengths in the 200 - 775 nm range) and emission (200 - 800 nm range) spectra were recorded at 120 nm/min scan rate, adjusting the slits at 4 nm.

Results

Definition and optimization of instrumental parameters with reference materials

In order to optimize the operating parameters for the spectrofluorometric detector to be used in the GPC analyses, 3D fluorescence spectra (x-axis: emission wavelength; y-axis: excitation wavelength; z-axis; intensity) of the two selected reference materials were recorded. The obtained fluorescence spectral map shows a maximum excitation at λ_{ex}=260 nm with a corresponding maximum emission centered at 335 nm (figure 1). These features of the fluorescence spectrum of polystyrene have been attributed to the emission from excimers formed between nearest neighbors pendant phenyl groups,[23-26] the fluorescence intensity being dependent on the molecular weight (MW).[27] In the case of LDPEox the maximum emission can again be obtained at λ_{ex}=260 nm, resulting in two main emission bands centred at 358 and 375 nm, together with a bathochromically shifted, broad shoulder above 400 nm (figure 2) that appears as a single and more intense band upon excitation at λ_{ex}=370 nm.

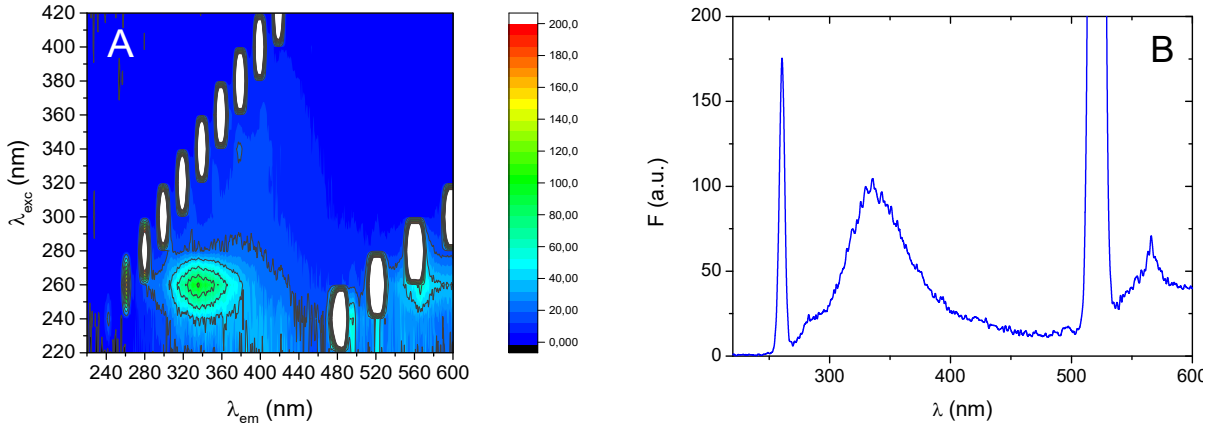

Figure 1. (A) 3D fluorescence spectral map the DCM extract of PS (x-axis = emission wavelength, y-axis = excitation wavelength, z-axis = intensity); (B) emission spectrum of a solution of PS in DCM with λ_{exc} = 260 nm.

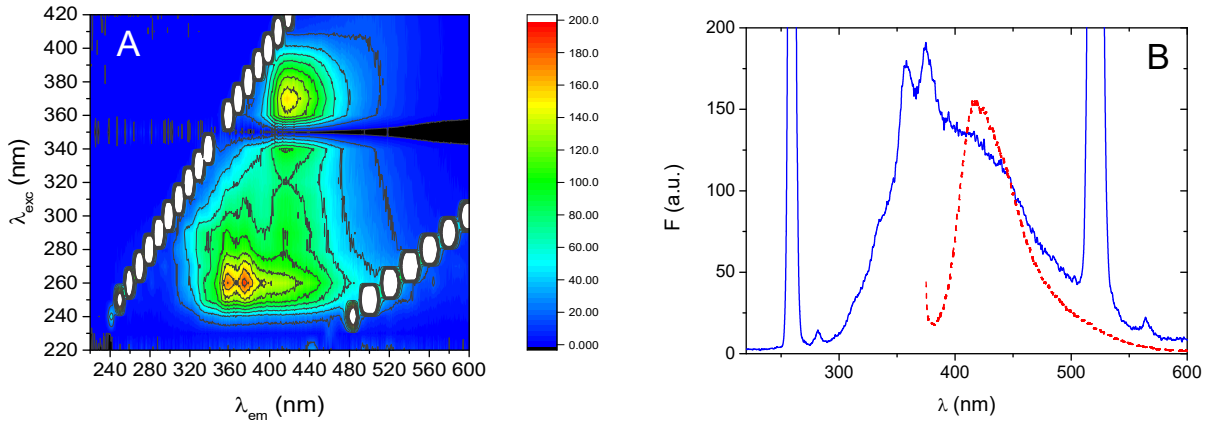

Figure 2. (A) 3D fluorescence spectral map the DCM extract of LDPEox (x-axis = emission wavelength, y axis = excitation wavelength, z-axis = intensity); (B) emission spectrum of a solution of LDPEox in DCM with λ_{exc} = 260 nm (—) or 370 nm (- -).

Photoluminescence of polyolefins is somewhat controversial,[28] having been associated with the presence of oxidized "impurities" such as carbonyl end groups,[29,30] α,β-unsaturated carbonyl (enone and dione types)[31] and dicarbonyl species. Photoluminescence and chemiluminescence properties of oxidized polyolefins have already been exploited for quantitative analyses because of their higher sensitivity with respect to e.g. FT-IR spectroscopy; the kinetics of thermo- and photo-oxidative degradation of polyolefins could thus be studied from the very onset, when only few oxidized groups are present.[32-35] In most cases, an initial decrease in the emission, ascribed to the loss of fluorescent additives (e.g. antioxidants) has been observed, followed by a substantial increase

closely related with the evolution of degradation processes.[34] Such post-oxidative luminescence has been generally attributed to the initial formation of α,β-unsaturated carbonyl and similarly oxygenated groups, followed by the development of more extended conjugated systems such as short polyene sequences that may or may not be conjugated to carbonyl groups;[36,37] the latter are typically excited at longer wavelengths (between 300 and 400 nm) with ensuing fluorescence at wavelengths exceeding 500 nm.[34,38]

In agreement with the cited literature, the 3D fluorescence spectrum of the LDPEox reference material used in this study shows a main emission centered at 420 nm with a tail extending up to 500 nm upon excitation at 370 nm. Thus the PS and LDPEox samples were used as the reference materials for setting up the operating conditions of a GPC apparatus equipped with fluorescence detector, with the aim of assessing the suitability and accuracy of the technique for the qualitative and semi-quantitative determination of naturally oxidized PS and polyolefins.

In figure 3 are reported the GPC traces recorded with a DAD detector at 261 nm from the analysis of the DCM-soluble fractions of the two reference materials and of the DCM extracts obtained from beach sand samples collected in the winter berm and dune sectors (samples G3040011 and G3040012, respectively) of a touristic seashore site in north Tuscany, Italy.[3]

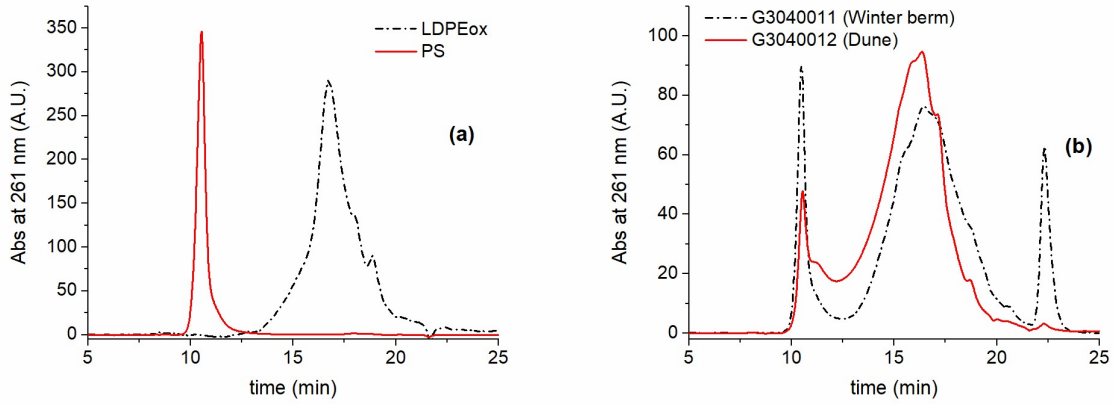

Figure 3. GPC traces recorded with DAD detector at λ=261 nm: (a) DCM-soluble fraction of LDPEox and from PS (whole sample) reference materials; (b) DCM extracts of the sand samples from the winter berm (sample G3040011) and dune (sample G3040012) sectors.

In figure 3a the GPC trace of LDPEox presents a single broad and structured peak at high retention times (r.t.) associated with low-to-medium MW fractions (as expected, since high MW polyolefins are insoluble in DCM); on the other hand the GPC trace of the reference PS is characterized by a single peak at lower r.t. (its narrowness being most likely an artifact caused by a MW distribution covering a range close to the exclusion limit of the GPC columns), indicating the almost exclusive

presence of high MW polymeric material. Indeed, the GPC traces from both sand DCM extracts (figure 3b) show the presence of both a narrow peak at low r.t. and a broad peak at high r.t., indicating the presence of both high and low-to-medium MW fractions, respectively.

The UV spectra collected with the DAD detector in correspondence with the narrow peak at low r.t. (structured absorption band with λ_{max}=262 nm and a secondary characteristic peak at λ=269 nm) and with the broad peak at high r.t. (broad absorption band with λ_{max} around 242 nm and a long tail extending up to nearly 400 nm) from the GPC fractionation of the two sand extracts matched quite well those recorded under the same conditions from the reference PS and LDPEox, respectively (figure 4).

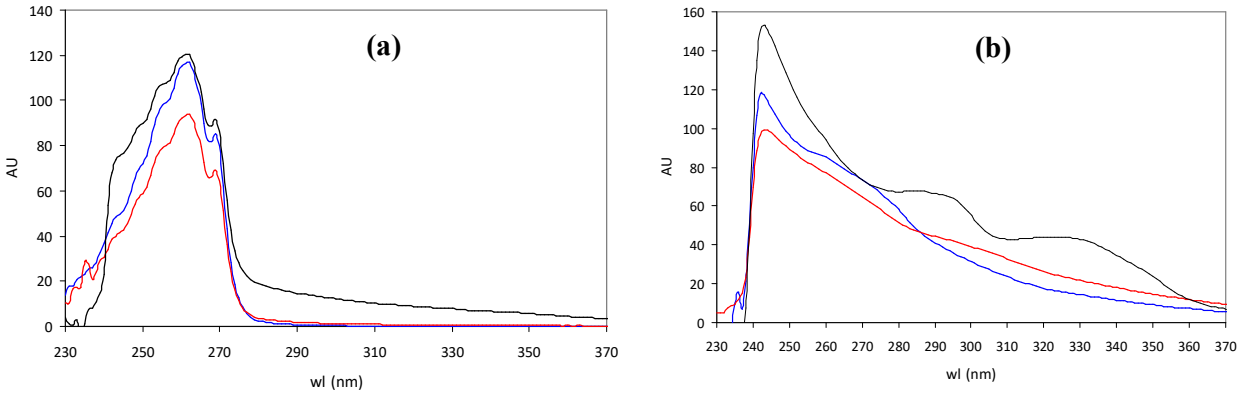

Figure 4. DAD UV spectra of GPC elution fractions of DCM extracts from test samples and reference materials recorded at 10.5 min (a) and 16.5 min (b) retention time. Black line: reference PS (A) and LDPEox (B) polymeric material; red line: winter berm sample; blue line dune sample.

In order to check the accuracy of the DAD detector for the evaluation of the concentrations of the two polymer types (PS and oxidized polyolefins) in real samples, two calibration curves were obtained by running GPC analysis of PS and LDPEox DCM solutions at different concentrations. The analyses, performed in triplicate for each concentration of the reference materials, gave a strictly linear relationship between concentration and DAD peak area within the explored range of 25-5500 mg/L for PS and of 720-7400 mg/L for LDPEox.

The GPC runs with the same reference PS and LDPEox solutions and with the two beach sand DCM extracts were then replicated in four subsequent experiments by setting up the fluorescence detector (FLD) at four different excitation/emission wavelengths combinations: 260/280 nm, 260/335 nm, 370/395 nm, and 370/420 nm. Representative GPC traces obtained from the same sample but with different FLD setup (excitation/emission wavelengths at 260/280 nm and 370/420 nm, respectively) are shown in figure 5.

In accordance with the fluorescence spectral map of the reference materials (figure 1 and figure 2), when the fluorescence detector was set at 260/280 nm excitation/emission wavelengths the

fluorescence contribution of LDPEox (DCM-soluble fraction) was found to be negligible, as opposed to the strong fluorescence response associated with PS materials (figure 5a-b). Such a clear-cut discrimination of the two polymeric materials was obtained neither by recording the emissions at 335 nm with the same excitation wavelength, nor with the FLD set at 370/385 nm excitation/emission. On the other hand, with the FLD set at 370/420 nm excitation/emission the fluorescent response of PS-like materials becomes negligible, while LDPEox and, more generally, oxidized polyolefins exhibit a residual fluorescence sufficient for their selective quantification (figure 5c-d).

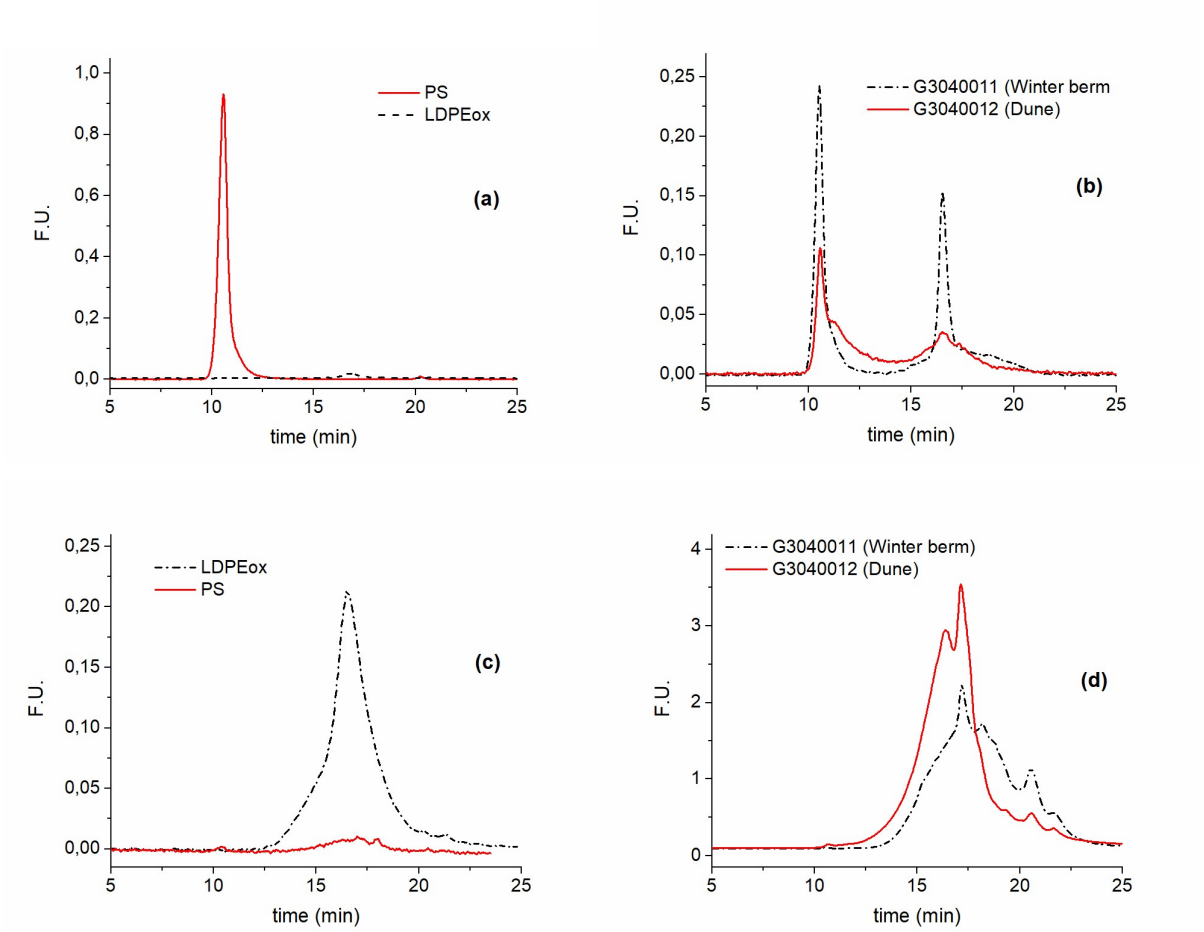

Figure 5. GPC traces recorded with different FLD set ups: with 260/280 nm excitation/emission wavelengths from LDPEox and PS reference materials (a) and from the DCM extracts of the beach sand samples from the winter berm and dune sectors (b); with FLD set up at 370/420 nm excitation/emission wavelength from LDPEox and PS reference materials (c) and from the DCM extracts of winter berm and dune samples (d).

Based on the above results, the 260/280 and 370/420 nm combinations of excitation/emission wavelengths can be considered as suitable to distinguish and recognize polystyrene-like materials from degraded and oxidized polyolefins within the same sample along with GPC separation.

To assess the accuracy of the detection also for the quantitative analysis of these two classes of polymeric materials, and more specifically for their determination as environmental contaminants extracted as DCM soluble fraction from coastal sand sediments, two distinct calibration curves were obtained by analyzing DCM solutions of the reference PS (5.51 - 0.033 mg/mL range) and DCM extracts of the reference LDPEox (4.33 - 0.57 mg/mL range) with the FLD set at 260/280 nm and 370/420 nm excitation/emission, respectively. In figure 6 are reported the linear fits of the calibration curves obtained by considering the GPC peak areas from the GPC/FLD traces.

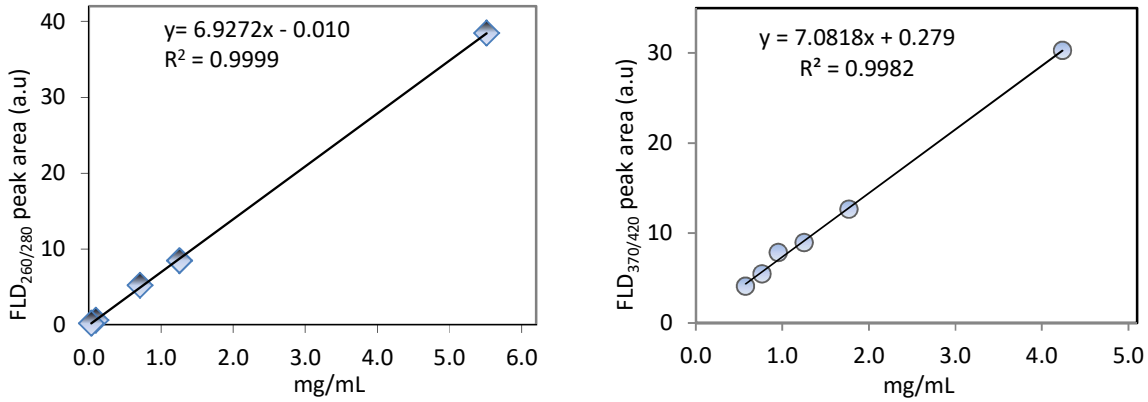

Figure 6. GPC calibration curve based on FLD detector. Left: reference PS (λ_{exc}=260 nm; λ_{em}=280 nm); right: reference LDPEox (λ_{exc}=370 nm; λ_{em}=420 nm).

It is worth pointing out that, although at a given wavelength the intensity of fluorescence emission $F=\phi_F(I-I_0)$ (where ϕ_F is the quantum yield, I_0 and I the incident and transmitted radiation, respectively) scales exponentially with the concentration C of the fluorophore along with equation 1,

$$\frac{I}{I_0} = e^{-2.3\,\varepsilon bC} \qquad (1)$$

(where ε and b are the molar absorption coefficient and the optical path, respectively), the linear approximation $I=I_0(1-2.3\varepsilon bC)$ that holds for equation 1 under conditions of negligible inner filter effect (low absorption coefficient at the excitation wavelength and low concentration) result in linearity of the response also for the fluorescence intensity, $F=2.3\phi_F I_0 \varepsilon bC$. These are the conditions normally used for analytical applications and that are found to apply in the systems investigated here.

It is worth pointing out that for LDPEox the calibration curve was built using what is actually a heterogeneous mixture of variously oxidized medium-to-low MW LDPE degradation products, that is, the fraction of LDPEox soluble in DCM, the latter being a very poor solvent for polyolefin-based plastics. Such mixture will contain very low MW fragments (up to a few thousand Da) soluble in DCM even if moderately oxidized, along with a higher MW fraction with a higher degree of oxidation, the latter being typically characterized by higher UV absorption and photoluminescence than the former. Therefore, the accuracy of a calibration based on the DCM-soluble fraction of a specific LDPEox sample used as a reference material is necessarily limited as a tool for quantitative determination of the DCM-soluble fraction of degraded polyolefins in general (POox), including LDPE, HDPE (high density polyethylene), PP, and similar semicrystalline olefin copolymers. However, since polyolefin solubility in a polar solvent such as DCM can be achieved only as a result of extensive generation of oxidized functional groups and chain scissions, using a LDPEox-based calibration curve was deemed as sufficiently accurate for quantitative determinations limited to the DCM-soluble fraction of any degraded polyolefin pool. In fact, such fraction is likely to present similar spectroscopic properties and fluorescence response, irrespective of the type of original undegraded polyolefin material.[39]

The experimental and calculated data from the quantitative analysis of the two environmental samples based on both DAD and FLD detection of the GPC eluates are reported in table 1.

Table 1. Content and composition of the DCM extracts from environmental sand samples calculated using the DAD and FLD calibration curves based on PS and LDPEox reference materials.

Sampling sector	Sample	Total extracts [(a)] (mg/kg)	High MW PS [(b)] (mg/kg)		Total PS (mg/kg)	POox [(c)] (mg/kg)
			DAD	$FLD_{260/280}$	$FLD_{260/280}$	$FLD_{370/420}$
Dune	G3040012	327.0	57.0±7.6	66.1±4.1	104.3±7.0	76.9
Winter berm	G3040011	18.7	6.1±1.5	5.7±0.5	8.4±1.0	3.3

[(a)] weighed amount of polymeric material extracted with DCM from 1 kg sand;

[(b)] from the lower r.t. GPC peak area (see reference 3);

[(c)] calculated from the calibration curve obtained using LDPEox as the reference material.

Concerning the analysis of PS content, a quantitative analysis based on the DAD detector was only possible for the high MW fraction consisting of nearly pure PS; for such fraction a good match of the results from the calculations based on the DAD and FLD detection was found. On the other hand, only the FLD detection allows to evaluate the total amount of PS since the DAD detector does not distinguish between PS and POox, both present in the low MW fraction. Concerning the POox

fraction, the figures obtained from the selective FLD detection of the GPC peak area with LDPEox calibration appears to largely underestimate the actual content according to the total amount of polymeric extracts determined by gravimetry. Such mismatch is likely to be the result of the presence of a seemingly large fraction of very low MW reduced hydrocarbon species such as natural waxes, heavy aliphatic hydrocarbon pollutants (e.g. from oil spillage), along with very low molecular weight polyolefin fragments possibly generated by extensive chain scission.

Conclusions

GPC chromatography with fluorescence detection (FLD) allows selective determination of hydrocarbon-based microplastics pollutants sampled from surface seawater and coastal sediments. The procedure involves using suitable excitation/emission wavelengths for the fluorometric detection of polystyrene (PS) and of the DCM-soluble fraction of degraded polyolefins (POox) upon GPC separation. Linear FLD response with concentration was found for both PS and LDPEox reference materials used as calibration standards. Accurate direct determination of PS can be achieved, while for polyolefins the analysis is limited to the DCM-soluble, highly degraded polyolefin fraction. In the latter case a lower accuracy may result from the intrinsic structural variability of the POox pool and from the environmental contamination by heavy hydrocarbons pollutants (e.g. from oil spillage). Nevertheless, the devised technique allows to perform with unprecedented accuracy a semi-quantitative evaluation of the microplastics pollutants from marine sediments, notably in combination with gravimetric determination of the DCM soluble fractions.

ACKNOWLEDGEMENTS

This work was supported by the University of Pisa [PRA 2017_17 project]

References

(1) Andrady, A. L. *Mar Mar. Pollut. Bull.* **2011**, *62*, 1596-1605.

(2) Cooper, D. A.; Corcoran, P. L. *Mar. Pollut. Bull.* **2010**, *60*, 650-654.

(3) Ceccarini, A.; Corti, A.; Erba, F.; Modugno, F.; La Nasa, J.; Bianchi, S.; Castelvetro, V. *Environ. Sci. Technol.* **2018**, *52*, 5634−5643.

(4) Duis, K.; Coors, A. *Environ. Sci. Eur.* **2016**, *28*, 2.

(5) Imhof, H. K.; Schmid, J.; Niessner, R.; Ivleva, N. P.; Laforsch, C. *Limnol. Oceanogr. Methods* **2012**, *10*, 524-537.

(6) Nuelle, M.-T.; Dekiff, J. H.; Remy, D.; Fries, E. *Environ. Poll.* **2014**, *184*, 161-169.

(7) Rocha-Santos, T.; Duarte, A. C. *Trends Anal. Chem.* **2015**, *65*, 47-53.

(8) Cole, M.; Webb, H.; Lindeque, P. K.; Fileman, E. S.; Halsband, C.; Galloway, T. S. *Sci. Reports* **2014**, *4*, 4528.

(9) Vianello, A.; Boldrin, A.; Guerriero, P.; Moschino, V.; Rella, R.; Sturaro, A.; Da Ros, L. *Estuar. Coast. Shelf Sci.* **2013**, *130*, 54-61.

(10) Song, Y. K.; Hong, S. H.; Jang, M.; Han, G. M.; Rani, M.; Lee, J.; Shim, W. J. *Mar. Pollut. Bull.* **2015**, *93*, 202-209.

(11) Harrison, J. P.; Ojeda, J. J.; Romero-Gonzalez, M. E. *Sci. Total Environ.* **2012**, *416*, 455-463.

(12) Kaeppler, A.; Windrich, F.; Laeder, M. G. J.; Malanin, M.; Fischer, D.; Labrenz, M.; Eichhorn, K.-J.; Voit, B. *Anal. Bioanal. Chem.* **2015**, *407*, 6791-6801.

(13) Fries, E.; Dekiff, J. H.; Willmeyer, J.; Nuelle, M.-T.; Ebert, M.; Remy, D. *Environ. Sci.: Processes Impacts* **2013**, *15*, 1949-1956.

(14) Fabbri, D.; Tartari, D.; Trombini, C. *Anal. Chim. Acta* **2000**, *413*, 3-11.

(15) Fabbri, D.; Trombini, C.; Vassura, I. *J. Chromatogr. Sci.* **1998**, *36*, 600-604.

(16) van Loon, W. M. G. M.; Boon, J. J.; de Groot, B. *Anal. Chem.* **1993**, *65*, 1728-1735.

(17) Audisio, G.; Bertini, F. *J. Anal. Appl. Pyrolysis* **1992**, *24*, 61-74.

(18) Duemichen, E.; Barthel, A.-K.; Braun, U.; Bannick, C. G.; Brand, K.; Jekel, M.; Senz, R. *Water Res.* **2015**, *85*, 451-457.

(19) Duemichen, E.; Eisentraut, P.; Bannick, C. G.; Barthel, A.-K.; Senz, R.; Braun, U. *Chemosphere* **2017**, *174*, 572-584.

(20) Ziccardi, L. M.; Edgington, A.; Hentz, K.; Kulacki, K. J.; Driscoll, S. K. *Environ. Toxicol. Chem.* 35 (2016) 1667–1676

(21) Harrison, J. P.; Sapp, M.; Schratzberger, M.; Osborn, A. M. *Mar. Technol. Soc. J.* **2011**, *45*, 12-20.

(22) Lobelle, D.; Cunliffe, M. *Mar. Pollut. Bull.* **2011**, *62*, 197-200.

(23) Torkelson, J. M.; Lipsky, S.; Tirrell, M.; Tirrell, D. A. *Macromolecules* **1983**, *16*, 326-330.

(24) Vala, M. T.; Haebig, J.; Rice, S. A. *J. Chem. Phys.* **1965**, *43*, 886-897.

(25) Torkelson, J. M.; Lipsky, S.; Tirrell, M. *Macromolecules* **1981**, *14*, 1601-1603.

(26) Hirayama, F. *J. Chem. Phys.* **1965**, *42*, 3163-3171.

(27) Ishii, T.; Handa, T.; Matsunaga, S. *Macromolecules* **1978**, *11*, 40-46.

(28) Allen, N. S.; Edge, M.; Holdsworth, D.; Rahman, A.; Catalina, F.; Fontan, E.; Escalona, A. M.; Sibon, F. F. *Polym. Degrad. Stab.* **2000**, *67*, 57-67.

(29) Charlesby, A.; Partridge, R. H. *Proc. R. Soc. A* **1965**, *283*, 312-328.

(30) Allen, N. S.; Homer, J.; McKellar, J. F. *J. Appl. Polym. Sci.* **1977**, *21*, 2261-2267.

(31) Allen, N. S.; Homer, J.; McKellar, J. F.; Wood, D. G. M. *J. Appl. Polym. Sci.* **1977**, *21*, 3147-3152.

(32) Jacques P. P. L., P. R. C. *Eur. Polym. J.* **1993**, *29*, 75-81.

(33) Steffen, R.; Wallner, G.; Rekstad, J.; Röder, B. *Polym. Degrad. Stab.* **2016**, *134*, 49-59.

(34) Grabmayer, K.; Wallner, G. M.; Beissmann, S.; Braun, U.; Steffen, R.; Nitsche, D.; Raeder, B.; Buchberger, W.; Lang, R. W. *Polym. Degrad. Stab.* **2014**, *109*, 40-49.

(35) Tiemblo, P.; Gòmez-Elvira, J. M.; Teyssedre, G.; Massine, F.; Laurent, C. *Polym. Degrad. Stab.* **1999**, *65*, 113-121.

(36) Jacques P. P. L., Poller, R. C. *Eur. Polym. J.* **1993**, *29*, 83-89.

(37) Osawa, Z.; Kuroda, H. *Polym. Photochem.* **1986**, *7*, 231-236.

(38) Grabmayer, K.; Wallner, G. M.; Beissmann, S.; Schlothauer, J.; Steffen, R.; Nitsche, D.; Raeder, B.; Buchberger, W.; Lang, R. W. *Polym. Degrad. Stab.* **2014**, *107*, 28-36.

(39) Chiellini, E.; Corti, A.; D'Antone, S.; Baciu, R. *Polym. Degrad. Stab*. **2006**, *91*, 2739-2747.